Biomineralization

DOI: 10.1002/anie.200703752

Mimicking Biosilicification: Programmed Coassembly of Peptide–Polymer Nanotapes and Silica**

*Stefanie Kessel, Arne Thomas, and Hans G. Börner**

Biological inorganic–bioorganic hybrid materials, from bones[1] to filaments of glass sponges[2,3] to shells of mollusks,[4] are high-performance composites with properties well-adapted to their purpose and frequently superior to synthetic mimics.[5,6] This is a result of defined hierarchical structures that are formed by self-assembly and templating processes facilitated by proteins, peptides, or polysaccharides.[7] Marine glass sponges, for instance the hexactinellid sponge *Euplectella* sp., are considered to be one of the most primitive animals in existence. However, they produce integrated composite materials with outstanding mechanical properties.[2,8] This material exhibits a rather complex design, thus ensuring the control of both mechanical and chemical interfaces between the different components to overcome the brittleness of the main constituent material, glass.[2] Inspired by the formation of bioglass filaments,[9] we report the peptide-directed silicification of self-assembled peptide–polymer nanotapes. The spontaneously formed reinforced silica fibers exhibit a distinct inner structure with six distinguishable levels of hierarchical order.

Proteins such as silaffin[10] from diatoms or silicatein[11] from glass sponges catalyze and guide the formation of silica from dilute silicic acid solution at neutral pH in vivo and in vitro.[12] Deming et al. pioneered the mimicking of the functions of such proteins by using poly(cysteine-*block*-lysine).[13] This approach was further broadened by applying other polypeptides and polypeptide derivatives.[14] In addition, several low-molecular-weight compounds containing α-amino acids were used to create chiral, mesoporous silica through sol–gel templating routes.[15]

In analogy to the formation of biological glass fibers, we encoded the structural and functional information in a fiberlike nanostructure, which was particularly designed to direct the silicification process (Figure 1). To access these functional nanotapes (Figure 1a), a peptide–polymer conjugate, which combines polyethylene oxide (PEO) with an oligopeptide segment, was synthesized and assembled as

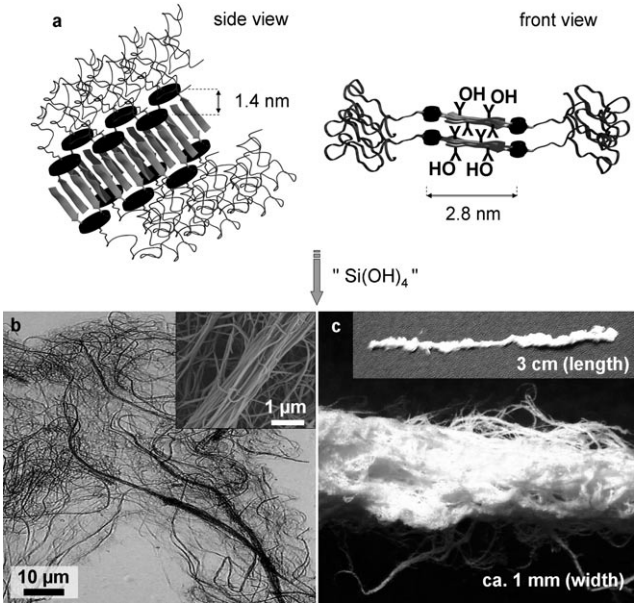

Figure 1. Spontaneous formation of silica composite fibers by the addition of "silicic acid" to a dilute solution of PEO–peptide nanotapes. a) Schematic representation of nanotapes with a functional peptide β-sheet core and a PEO shell. b) Optical microscopy image of the composite fibers; inset: SEM image of proto-composite fibers in bundles. c) Macrocomposite fibers resulting in macroscopic threads.

described previously (see Supporting Information).[16] The resulting PEO–peptide nanotapes have a peptide β-sheet core and a PEO shell. The latter shields the functional peptide core, thus preventing lateral interactions and limiting the organization on the structural level of the nanotapes. These exhibit a cross-section of 15 × 1.4 nm (width × height), lengths of up to 2 μm, and chemically encode information as a result of well-defined functional patches that run along the center of the tapes (Figure 1a). These patches contain precisely positioned hydroxy groups from threonine residues, which are essential to direct the formation of silica, as proposed for biosilicification processes.[17–20]

The addition of prehydrolyzed tetramethoxysilane (TMOS, 1 h, pH 1.1), as a common precursor of silica sol–gel chemistry, to a dilute solution of the PEO–peptide nanotapes in ethanol results in the spontaneous precipitation of macroscopic fibers within a few seconds (Figure 1b). These fibers show lateral dimensions of about 400 nm to 2 μm and can be easily removed from solution by using tweezers or filtration. UV spectroscopy of the cleared solution indicated the removal of about 85% of the PEO–peptide nanotapes. Fourier-transform infrared spectroscopy (FTIR) of the isolated fibers confirmed the presence of both unaffected PEO–

[*] S. Kessel, Dr. A. Thomas, Dr. H. G. Börner
Max Planck Institute of Colloids and Interfaces
Department of Colloids
Am Mühlenberg 1, 14476 Golm (Germany)
Fax: (+49) 331-567-9502
E-mail: hans.boerner@mpikg.mpg.de
Homepage: http://www.mpikg.mpg.de/kc/boerner/

[**] This work was supported by the German Research Foundation (DFG) through the Emmy Noether Program (BO 1762/2-2 and -3) and the Max Planck Society. We are grateful to M. Antonietti, T. Brezesinski, M. Groenewolt, H. Gupta, and Erich C.

Supporting information for this article is available on the WWW under http://www.angewandte.org or from the author.

peptide nanotapes and silica in the fibers (see Supporting Information). The composition of representative composite fibers was quantified by thermogravimetric analysis (TGA), which showed a ratio of about 59:41 wt % inorganic to organic material.

A detailed structural analysis of the inorganic–organic composite fibers indicates the presence of distinct hierarchical structure levels. Scanning electron microscopy (SEM) images reveal the formation of proto-composite fibers with rather uniform widths of 95 ± 15 nm and lengths of several tens of micrometers (Figure 1b inset and Supporting Information). These proto-composite fibers show a high tendency to form bundles, which leads to macroscopic composite fibers and bundles of such, spanning diameters from 400 nm to 2 μm. Depending on the conditions, entanglement similar to the classic spinning process of wool can be observed, in which composite fiber bundles build up macroscopic fiber threads with diameters of up to 1 mm and lengths of about 3 cm (Figure 1c).

The outstanding performance of fiber-reinforced biomaterials and synthetic-fiber composites results from the orientation of the fiber elements along the stress–force vectors.[1,5] Thus, it is essential to investigate the orientation of the PEO–peptide nanotapes within the proto-composite fibers. This was accessed by calcining the composite fibers at 550 °C, which causes the quantitative decomposition of the organic components.

Figure 2a shows an SEM image of the remaining porous silica fibers. The silica network appears to be sufficiently

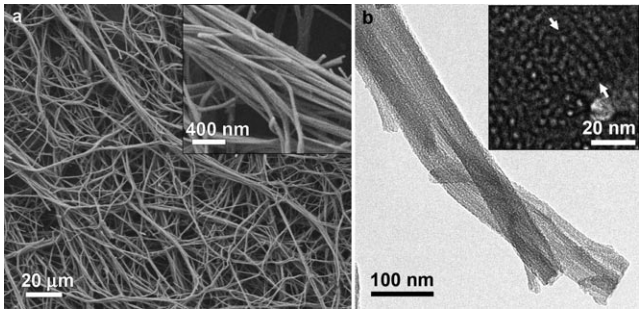

Figure 2. Porous silica fibers formed by calcination of the composite fibers. a) SEM image of porous silica fibers with preserved structure and hierarchical organization. b) TEM image of calcined proto-composite fibers with highly organized inner structure; inset: microtome cut of embedded silica fibers, which shows the cross-section of the pores and pore stacking (arrows) in the materials.

stable not to collapse during heating. Transmission electron microscopy (TEM) of the silica fibers enables visualization of the pore organization and hence gives insight into the orientation of the PEO–peptide nanotapes within the non-calcined proto-composite fibers. In Figure 2b, well-aligned pores can be seen, which are parallel over several hundreds of nanometers (see Supporting Information). The inner diameter of these pores is 3 ± 0.5 nm and the pore-to-pore distances are in the range of 5.6 ± 0.6 nm, as determined from microtome cuts of embedded silica fibers (Figure 2b inset). The pore-to-pore distance was confirmed by small-angle X-ray scattering with a *d* spacing of 5.8 ± 0.2 nm (see Supporting Information).

The pore diameter correlates with the dimensions of the peptide core of the PEO–peptide nanotapes (calculated cross-section $= 2.8 \times 1.4$ nm). N_2 sorption measurements suggest the presence of uniform mesopores with diameters of ca. 2.9 nm and micropores, which corresponds to the templating of the peptide core and single PEO chains, respectively. Furthermore, Brunauer–Emmett–Teller (BET) evaluation revealed a specific surface area of ca. $870\ m^2 g^{-1}$ (Supporting Information).

Given the suggested process of biosilicification,[19] a structure-directed silicification mechanism can be proposed: TMOS was used as the silica source and the preceding hydrolysis was performed at a pH value close to the isoelectric point of monosilicic acid. Thus, the hydrolysis of the organic precursor is fast, whereas condensation of the original silicic acid remains slow. It was expected that the apparent pH would increase to ca. 4.5, as a result of dilution effects, if prehydrolyzed TMOS was added to the PEO–peptide nanotape solution. Hence, the silica species formed might be charged, making electrostatic interactions with the partially cationic peptide β sheet of the nanotapes feasible.[10]

Moreover, hydrogen bonding and hydrophobic entropy effects probably drive the preferential adsorption of "silicic acid" on the threonine-rich peptide faces. This hypothesis is supported by biosilicification processes of diatoms, in which enrichment of silicic acid on either cationic protein segments or hydroxy-rich β sheets induces protein-directed silicification.[10,19,20] Furthermore, computational models suggest a low-energy reaction pathway for β-sheet-facilitated condensation of silicic acid that is adsorbed on hydroxy groups of rather hydrophobic β-sheet faces.[17] A dominating contribution of the PEO shell to the primary silicification was excluded by control experiments, in which the PEO–peptide nanotapes were substituted by Pluronic P123 (PEO-PPO-PEO block copolymer; PPO = polypropylene oxide). This experiment highlights the significance of the peptide segments, because Pluronic does not induce silica precipitation or enhanced condensation under similar conditions. However, the exact mechanism of enrichment and partitioning of silicic acid within the PEO-peptide nanotapes will be studied by NMR spectroscopy.

As the peptide core of the nanotapes apparently has a prominent effect on the silicification, it is likely that silica condensation occurs on both sides of the solvent-exposed β-sheet faces of the nanotapes, thus generating proto-composite tapes with "sticky", hydrated silica patches (Figure 3a). In a synergistic self-assembly process the sticky mesogens organize primarily into stacks of multiple nanotapes (Figure 3b, Figure 2b inset). Here, the peptide controls the silica condensation while the silica itself acts as "glue" between the nanotapes and induces aggregation, which in turn is guided by the stiffness and anisotropy of the proto-composite tapes. Probably in a secondary assembly step, small stacks aggregate laterally at their PEO-grafted interfaces and remaining silica condenses within the PEO chains, which stabilizes the resulting proto-composite fibers (Figure 3c, Figure 2b). It is important to note that the removal of the

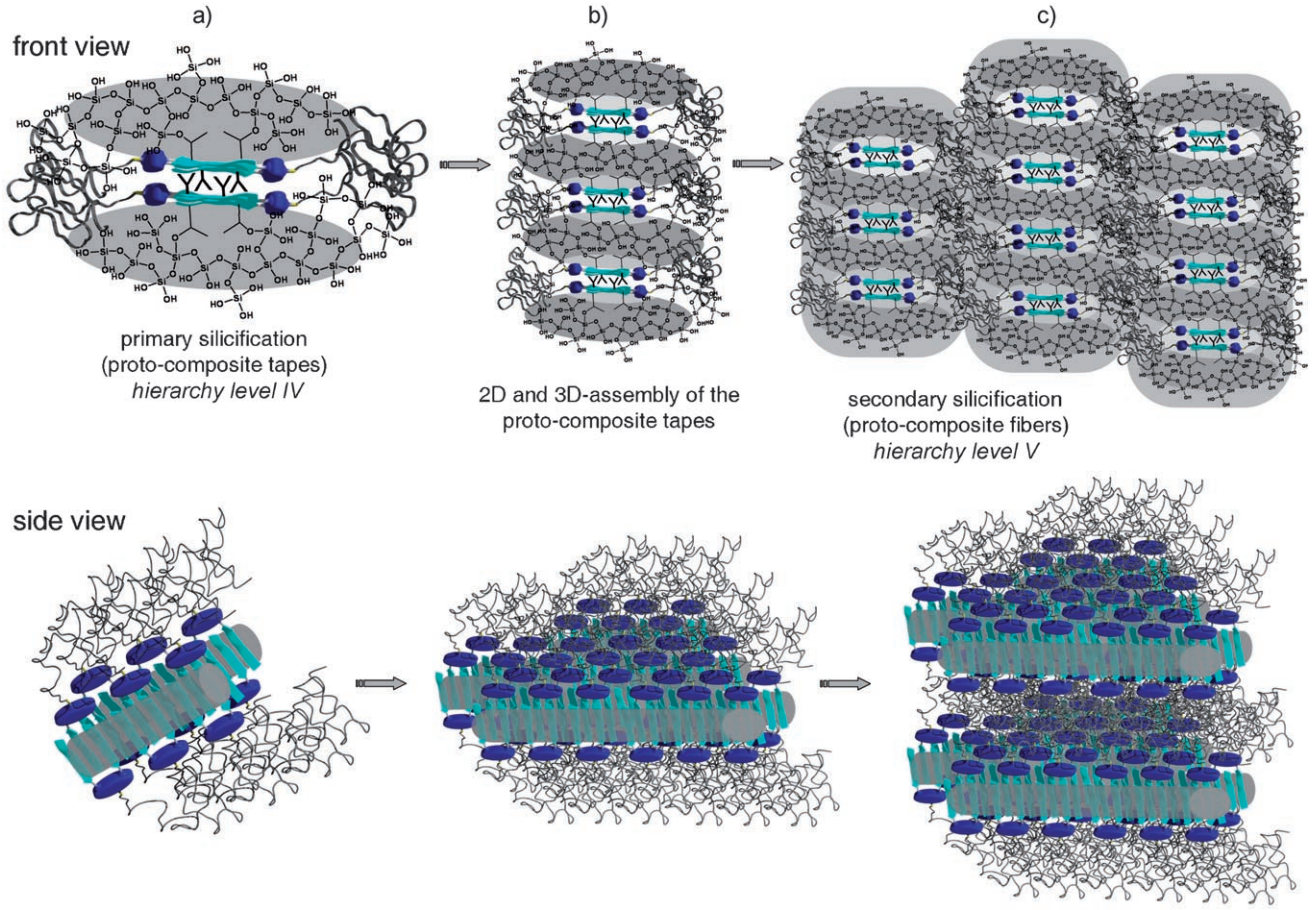

Figure 3. Proposed structure-directed silicification mechanism. The formation of silica is indicated by the gray areas, and the sizes of the structures are not drawn to scale for clarity.

PEO shell would lead to strong lateral interactions between the peptide tapes, and hence a substantial alteration of the silicification process can be expected.

The cooperative nature of the artificial silicification process allows for the rapid production of complex composite fibers with six distinguishable levels of hierarchical order. These were classified as the peptide–polymer conjugate (hierarchy level I, hydrodynamic radius $R_h \approx 5$ nm), which forms nanotapes with a single β-sheet core (hierarchy level II)[16] and eventually a double β-sheet core (hierarchy level III, cross-section 15×1.4 nm; see Supporting Information). Furthermore, the composite material is composed of proto-composite tapes (hierarchy level IV, cross-section 15×3 nm). The anisotropic self-assembly of these tapes leads to proto-composite fibers (hierarchy level V, width ca. 95 nm) that tend to form bundles (hierarchy level VI, width 0.1–2 μm). The entanglement of such bundles, which form threads up to 1 mm in width, cannot be considered as a hierarchy level because of the absence of a uniform assembly motif.

Biological silica fibers of glass sponges are construction materials; hence, the mechanical properties of the biomimetic composite fibers were investigated. Nanoindentation experiments on dried composite fibers revealed excellent properties of the material, with an indentation hardness of 0.99 ± 0.2 GPa that reached about one third of the hardness of natural sponge spicules (*Rosella racovitzea*) and about 13% that of optical glass fibers.[8] The excellent performance of the biocomposites results from the interplay of hardness and elasticity. A reduced indentation modulus of the biomimetic composite fibers of about 10 GPa results in a fiber with four times higher elasticity when compared to sponge fibers, or even approximately seven times more elastic than synthetic glass fibers. Compared to naturally occurring sponge spicules, the structure of the biomimetic composite fibers has an increased elasticity, which can be correlated to the increased amount of organic fibers. These results highlight the fact that precise control over structure is a key factor in biological and biomimetic materials, which allows the modulation of material properties over a broad range.

In conclusion, the hierarchical structure of biosilica fibers is controlled by proteins, and hence we have presented a biomimetic approach in which not only the composition and structure of the composite material were mimicked, but also the peptide-guided synthesis. Well-defined composite fibers with hierarchical design and interesting mechanical properties were obtained by the directed coassembly of functional PEO–peptide nanotapes with silica. Potentially, this approach advents the synthesis of novel silica materials with purpose-defined structures and adjustable properties.

Experimental Section

Descriptions of the experimental procedures, analytical methods, and instrumentation are provided as Supporting Information.

Received: August 15, 2007
Published online: October 24, 2007

Keywords: biomimetic synthesis · biomineralization · mesoporous materials · nanostructures · self-assembly

[1] P. Fratzl, H. S. Gupta, E. P. Paschalis, P. Roschger, *J. Mater. Chem.* **2004**, *14*, 2115.
[2] J. Aizenberg, J. C. Weaver, M. S. Thanawala, V. C. Sundar, D. E. Morse, P. Fratzl, *Science* **2005**, *309*, 275.
[3] J. C. Weaver, D. E. Morse, *Microsc. Res. Tech.* **2003**, *62*, 356.
[4] Y. Levi-Kalisman, G. Falini, L. Addadi, S. Weiner, *J. Struct. Biol.* **2001**, *135*, 8.
[5] J. E. Gordon, G. Jeronimidis, M. O. W. Richardson, *Philos. Trans. R. Soc. London Ser. A* **1980**, *294*, 545.
[6] M. F. Ashby, L. J. Gibson, U. Wegst, R. Olive, *Proc. R. Soc. London Ser. A* **1995**, *450*, 123.
[7] E. Dujardin, S. Mann, *Adv. Mater.* **2002**, *14*, 775.
[8] M. Sarikaya, H. Fong, N. Sunderland, B. D. Flinn, G. Mayer, A. Mescher, E. Gaino, *J. Mater. Res.* **2001**, *16*, 1420.
[9] G. Croce, A. Frache, M. Milanesio, L. Marchese, M. Causa, D. Viterbo, A. Barbaglia, V. Bolis, G. Bavestrello, C. Cerrano, U. Benatti, M. Pozzolini, M. Giovine, H. Amenitsch, *Biophys. J.* **2004**, *86*, 526.
[10] N. Kröger, R. Deutzmann, M. Sumper, *Science* **1999**, *286*, 1129.
[11] K. Shimizu, J. Cha, G. D. Stucky, D. E. Morse, *Proc. Natl. Acad. Sci. USA* **1998**, *95*, 6234.
[12] J. N. Cha, K. Shimizu, Y. Zhou, S. C. Christiansen, B. F. Chmelka, G. D. Stucky, D. E. Morse, *Proc. Natl. Acad. Sci. USA* **1999**, *96*, 361.
[13] J. N. Cha, G. D. Stucky, D. E. Morse, T. J. Deming, *Nature* **2000**, *403*, 289.
[14] a) S. V. Patwardhan, N. Mukherjee, S. J. Clarson, *J. Inorg. Organomet. Polym.* **2001**, *11*, 193; b) F. Rodriguez, D. D. Glawe, R. R. Naik, K. P. Hallinan, M. O. Stone, *Biomacromolecules* **2004**, *5*, 261; c) S. V. Patwardhan, S. J. Clarson, *J. Inorg. Organomet. Polym.* **2003**, *13*, 49; d) K. M. Hawkins, S. S. S. Wang, D. M. Ford, D. F. Shantz, *J. Am. Chem. Soc.* **2004**, *126*, 9112; e) M. M. Tomczak, D. D. Glawe, L. F. Drummy, C. G. Lawrence, M. O. Stone, C. C. Perry, D. J. Pochan, T. J. Deming, R. R. Naik, *J. Am. Chem. Soc.* **2005**, *127*, 12577; f) E. G. Bellomo, T. J. Deming, *J. Am. Chem. Soc.* **2006**, *128*, 2276.
[15] a) S. Che, Z. Liu, T. Ohsuna, K. Sakamoto, O. Terasaki, T. Tatsumi, *Nature* **2004**, *429*, 281; b) Y. G. Yang, M. Suzuki, H. Fukui, H. Shirai, K. Hanabusa, *Chem. Mater.* **2006**, *18*, 1324; c) Y. Yang, M. Suzuki, S. Owa, H. Shirai, K. Hanabusa, *J. Am. Chem. Soc.* **2007**, *129*, 581.
[16] D. Eckhardt, M. Groenewolt, E. Krause, H. G. Börner, *Chem. Commun.* **2005**, 2814.
[17] K. D. Lobel, J. K. West, L. L. Hench, *Mar. Biol.* **1996**, *126*, 353.
[18] a) C. C. Harrison, *Phytochemistry* **1996**, *41*, 37; b) D. M. Swift, A. P. Wheeler, *J. Phycol.* **1992**, *28*, 202.
[19] T. Coradin, P. J. Lopez, *ChemBioChem* **2003**, *4*, 251.
[20] R. E. Hecky, K. Mopper, P. Kilham, E. T. Degens, *Mar. Biol.* **1973**, *19*, 323.

